Particle-in-cell simulation of ion energy distributions on an electrode by applying tailored bias waveforms in the afterglow of a pulsed plasma

Paola Diomede,[a)] Demetre J. Economou,[b)] and Vincent M. Donnelly[c)]
Plasma Processing Laboratory, Department of Chemical and Biomolecular Engineering, University of Houston, Houston, Texas 77204-4004, USA

A Particle-in-Cell simulation with Monte Carlo Collisions (PIC-MCC) was conducted of the application of tailored DC voltage steps on an electrode, during the afterglow of a capacitively-coupled pulsed-plasma argon discharge, to control the energy of ions incident on the counter-electrode. Staircase voltage waveforms with selected amplitudes and durations resulted in ion energy distributions (IED) with distinct narrow peaks, with controlled energies and fraction of ions under each peak. Temporary electron heating at the moment of application of a DC voltage step did not influence the electron density decay in the afterglow. The IED peaks were "smeared" by collisions, especially at the higher pressures of the range (10–40 mTorr) investigated. © *2011 American Institute of Physics*. [doi:10.1063/1.3573488]

I. INTRODUCTION

Control of the ion energy distribution (IED) and ion angular distribution (IAD) on the substrate is critical for plasma processing.[1] The ion energy must be high enough to promote ion-assisted chemistry, but not excessively high so that selectivity is preserved and substrate damage does not occur. In addition, ions must be highly directional along the normal to the substrate, so that anisotropic etching of high aspect ratio features may be obtained. Ion directionality is improved in the absence of ion-neutral collisions in the sheath. This necessitates low pressure operation such that the ion mean free path is much longer than the sheath thickness.

The energy of ions bombarding the substrate depends on the sheath voltage, which in turn is influenced by any bias applied to the substrate. The application of substrate bias has therefore been used to control the ion energy distribution (IED). The most common bias voltage waveform is sinusoidal, resulting (for a collisionless sheath) in a bimodal IED.[2–4] The controlling parameter is $\tau_i/\tau_{rf} = (3s\omega)/(2\pi)[M/(2eV_s)]^{1/2}$ the ratio of the ion transit time through the sheath to the period of the applied RF.[2] Here, s, ω, M, and V_s are time-average sheath thickness, applied field angular frequency, ion mass, and time-average sheath voltage, respectively. When $\tau_i/\tau_{rf} \ll 1$, ions respond to the instantaneous sheath voltage, and the IED has a large energy spread. When $\tau_i/\tau_{rf} \gg 1$, ions respond to an average ("damped") sheath voltage, and the IED becomes narrow. The width of the distribution may be decreased by increasing the frequency of the applied field. However, when the frequency is too high, the RF wavelength becomes comparable to the substrate dimension, resulting in nonuniform voltage distribution across the substrate. In the presence of ion-neutral collisions in the sheath the IED exhibits multiple peaks.[5]

Recently, there have been several reports on the application of tailored voltage waveforms to better control the IED.[6–8] Wendt and co-workers[6,7] applied a low frequency impulse waveform or a square waveform on a substrate in a continuous wave (cw) plasma to obtain a peaked IED. The flat topped square waveform had to be given the right slope to account for charging of nonconductive substrates, and still yield a nearly constant sheath potential, and thus a nearly monoenergetic IED. A similar approach was used by Kudlacek *et al.*[8] The effect of substrate charging in influencing the required voltage waveform was studied. Agarwal and Kushner[9] and Rauf[10] investigated computationally the effect of nonsinusoidal bias voltage waveforms on the IED on the substrate in cw plasmas and, in turn, on etch rate and selectivity.

In this work, a Particle-In-Cell simulation with Monte Carlo Collisions (PIC-MCC) was performed to study the effect of tailored bias voltage waveforms on the IED on the substrate electrode. Specifically, a staircase positive DC bias with variable voltage levels was applied for a specified time window on the counter-electrode, during the afterglow of a power-modulated capacitively-coupled plasma. This work (a) presents a systematic study of the effect of DC bias on the IED, (b) examines the influence of ion-neutral collisions on the IED, and (c) discusses some details of the modification of the plasma dynamics due to the applied bias.

II. SIMULATION MODEL

Simulations were performed using a one-dimensional PIC code, XPDP1.[11] A capacitively-coupled parallel plate (plate separation 6 cm) argon plasma was simulated with a uniform background gas density of 1.9×10^{14} cm^{-3} (corresponding to 10 mTorr at 500 K). A radio frequency (RF) potential $V = 300 \sin(2\pi ft)$ (in V, where $f = 13.56$ MHz) was applied to the upper electrode, while the lower substrate electrode was grounded (Fig. 1). The peak RF potential was square-wave modulated with a frequency of 10 kHz and duty cycle of 50%. This arrangement resulted in 50 μs of plasma

a)Electronic mail: padiomede@gmail.com.
b)Electronic mail: economou@uh.edu.
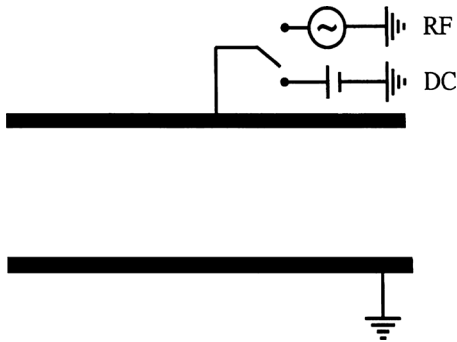c)Electronic mail: vmdonnelly@uh.edu.

FIG. 1. Schematic of a capacitively-coupled plasma reactor. Radio frequency power (during plasma ON) or a DC bias voltage (during plasma OFF) was applied to the upper electrode (boundary electrode), while the lower (substrate) electrode was grounded. Ion energy distributions were calculated on the lower electrode.

ON (active glow) and 50 μs of plasma OFF (afterglow), during each power modulation cycle. There was no DC self-bias developed during the active glow, due to the symmetry of the discharge. Twenty μs into the afterglow (RF power OFF), a tailored positive DC bias voltage (*boundary voltage*) was applied to the upper electrode (Fig. 2), to raise the plasma potential and expel positive ions out of the plasma. Singly charged argon positive ions and electrons were considered in the PIC simulation. Elastic electron scattering, excitation and ionization, as well as ion–neutral collisions (both scattering and charge exchange) were included.[12] The common restrictions on time step and grid size of the PIC simulation were observed.[13] The standard leap frog scheme was used to advance particles,[13] and the null collision technique was used for Monte Carlo collisions.[12] The secondary electron emission coefficient due to ion bombardment was set at 0.02. A limited number of simulations at a plasma excitation frequency of 60 MHz (300 V peak RF, 10 mTorr, 500 K) were also performed.

For a given set of operating conditions, a cw RF simulation was first run to reach a periodic steady-state.[14] For 13.56 MHz power, this required ~1000 RF cycles. The RF voltage was then turned OFF starting the afterglow. Application of the DC bias voltage commenced 20 μs into the afterglow, until the end of the afterglow (Fig. 2). The plasma ON, plasma OFF, DC ON, DC OFF cycle was repeated ~10 times to reach a periodic steady-state of the pulsed plasma. After that, time-averaged ion energy distributions
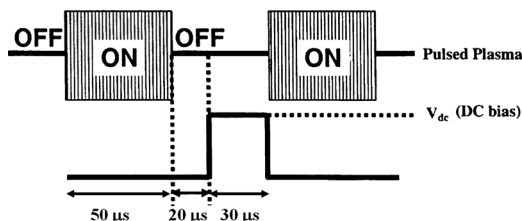
FIG. 2. A pulsed plasma was created by repeatedly switching radio frequency power ON for 50 μs and OFF for 50 μs. Twenty μs into the afterglow (RF power OFF), a DC bias voltage was applied until the end of the afterglow. The DC voltage was either a single step or a double step "staircase" (not shown in Fig. 2).

were collected on the substrate (grounded) electrode for 5 cycles, in order to reduce statistical noise. The substrate and supporting electrode were assumed conductive, preventing any possible charging effects.

III. RESULTS AND DISCUSSION

A. Ion energy distributions without bias

Figure 3 shows the IEDs obtained in a continuous wave (cw) discharge (Figure 3(a)), and in a pulsed discharge (Figure 3(b)), without the application of DC bias. In the cw plasma, the characteristic bimodal distribution is obtained, centered around 140 eV, with a fairly narrow width (the corresponding τ_i/τ_{rf} ~15). The location of the composite peak is rather well defined close to half of the applied peak voltage. The tail of the IED to the left of the main peak is due to ion-neutral collisions. Under these conditions, the ion mean free path λ_i is ~0.5 cm, commensurate with the time-average sheath width of $s \sim 1$ cm. This results in a significant collision probability $P_c = 1 - exp(-s/\lambda_i)$ of ~40%. The multiple peaks in the IED to the left of the main feature are due to the creation of cold ions by charge exchange collisions combined with rf modulation of the sheath electric field (see p. 446 of Ref. 1). When the plasma is pulsed (still without any DC bias), the bimodal IED is retained, originating from the power ON fraction of the cycle. However, a new peak
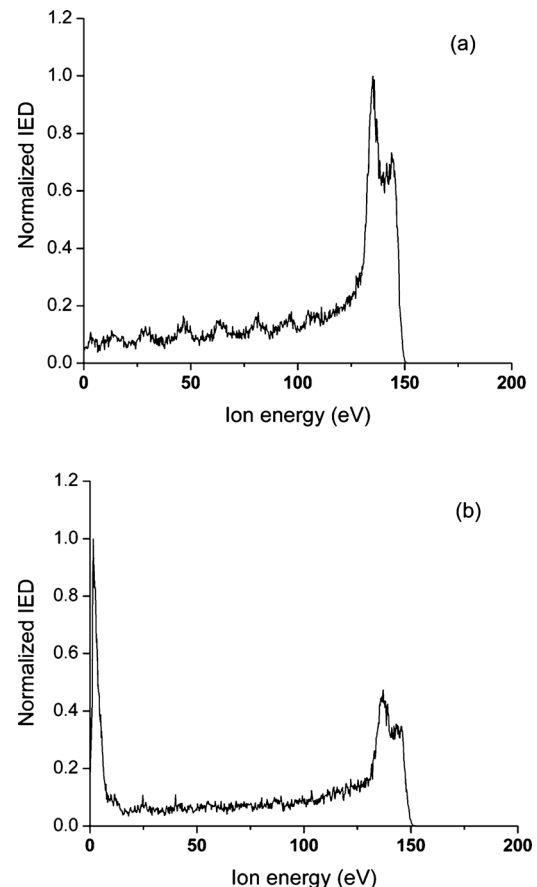
FIG. 3. (a) Ion energy distribution (IED) in a continuous wave (cw) plasma. (b) IED in a pulsed plasma (50 μs power ON, 50 μs power OFF). For both (a) and (b) the pressure was 10 mTorr and the gas temperature was 500 K.

appears at very low energies, <10 eV, corresponding to ions bombarding the substrate during the afterglow. After the plasma is turned OFF, the sheath potential collapses within a few microseconds, yielding very low ion bombardment energy during the afterglow. Ions with energy below 10 eV are very ineffective in promoting etching reactions.

B. Ion energy distributions with DC bias

1. Tailored staircase DC bias

The focus of this work was to investigate the effect of tailored DC bias voltages, applied to the boundary electrode during the afterglow, on the ion energy distribution (IED) at the substrate electrode. Figure 4 shows a "staircase" profile with two DC voltage levels. A voltage of 50 V is applied at $t = 70$ μs (i.e., 20 μs into the afterglow) for a specified time duration (5, 10, 15, 20, and 25 μs), followed by a voltage of 100 V applied for the remainder of the afterglow (i.e., for 25, 20, 15, 10, and 5 μs, respectively). Here time $t = 0$ refers to the start of the active glow (plasma ON). In each case, the resulting IED (Fig. 5), consists of two new distinct peaks around 50 and 100 eV, corresponding to the two DC bias voltage levels, superimposed on the IED of Fig. 3(b). A similar result was obtained by Xu et al.[15] for the case of a single DC voltage step applied in the afterglow. The fraction of ions in the 50 eV peak increases as the duration of the application of the corresponding voltage increases. Thus, the new peak locations and fraction of ions in each peak can be controlled by the level of the applied voltages and their duration. The fraction of ions under the composite peak corresponding
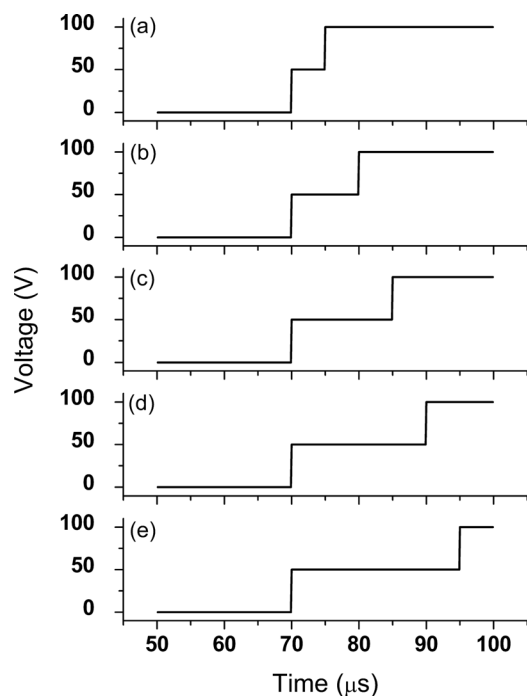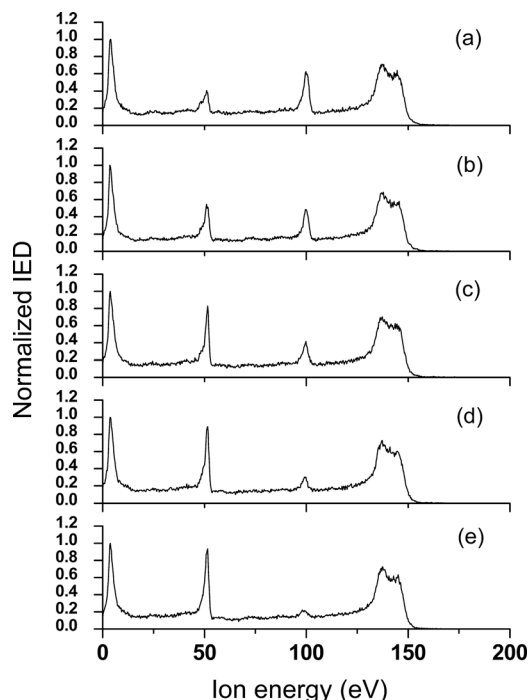

FIG. 5. Normalized ion energy distributions corresponding to the voltages of Fig. 4.

to the plasma ON fraction of the cycle (centered at ~140 eV) can be controlled by varying the duty cycle of the pulsed plasma. The peak broadening is due to the decay of the plasma potential during the time window over which the DC bias is applied, and also due to ion collisions. The IED tail to the left of each peak (except the very low energy peak) is due to ion-neutral collisions as well. IED computed with ion-neutral collisions intentionally turned off, under otherwise the same conditions, showed no tail to the left of the peaks.

In Fig. 5, the IEDs were time-averaged over the entire pulsed plasma cycle, i.e., over 100 μs. Figure 6 shows IEDs obtained by averaging over fractions of a cycle. Specifically, the IEDs shown in Fig. 6(a), 6(b), 6(c), and 6(d), respectively, correspond to averages over the plasma ON time (0–50 μs), afterglow without any DC bias (50–70 μs), afterglow with 50 V DC applied (70–85 μs) and afterglow with 100 V DC applied (85–100 μs). This result reinforces the fact that the "complete" IED (e.g., Fig. 5(c)) is a superposition of the peaks obtained over the different time windows that compose a full pulsed plasma cycle.

In another simulation, a staircase voltage was again applied, with the lower voltage level at 50 V, keeping the bias starting time and the bias window constant. The higher voltage level was varied (100, 200, or 300 V, see Fig. 7). The resulting IEDs (Fig. 8) again show two new distinct peaks superimposed on the IED without DC bias (that of Fig. 3(b)). The separation of the new peaks can be controlled by the levels of the applied voltage. In contrast to Fig. 5, the fraction of ions under each new peak is a weak function of the applied voltage levels (it is rather controlled by the duration of each voltage). The higher energy peak (at 100, 200, and 300 V) is progressively broadened, as the sheath becomes thicker for higher applied voltages.
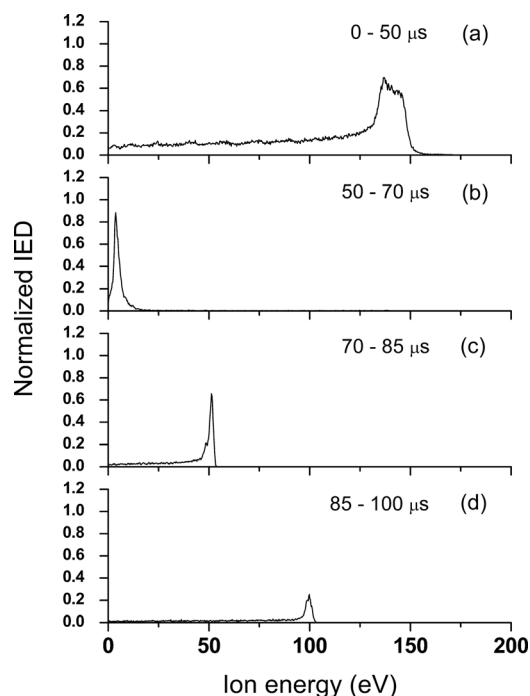

FIG. 4. Staircase DC bias voltage applied in the afterglow. Time $t = 50$ μs refers to the start of the afterglow (Plasma OFF). A 50 V DC step was applied starting 20 μs into the afterglow (at $t = 70$ μs), followed by the application of a 100 V DC (a) 5 μs, (b) 10 μs (c) 15 μs (d) 20 μs and (e) 25 μs later. The pressure was 10 mTorr and the gas temperature was 500 K.

FIG. 6. Normalized ion energy distributions obtained by time-averaging over different time windows during a pulsed plasma cycle. (a) 0–50 μs (plasma ON), (b) 50–70 μs (afterglow without bias), (c) 70–85 μs (afterglow with 50 V DC bias), and (d) 85–100 μs (afterglow with 100 V DC bias). The DC voltage applied in the afterglow was as in Fig. 4(c). The pressure was 10 mTorr and the gas temperature was 500 K.

2. Effect of pressure

To analyze the effect of pressure on the ion energy distribution, simulations were performed at three different pressures (10, 20, and 40 mTorr), with a single-step DC voltage (with strength of 50, 100, 200, or 300 V) applied 20 μs into
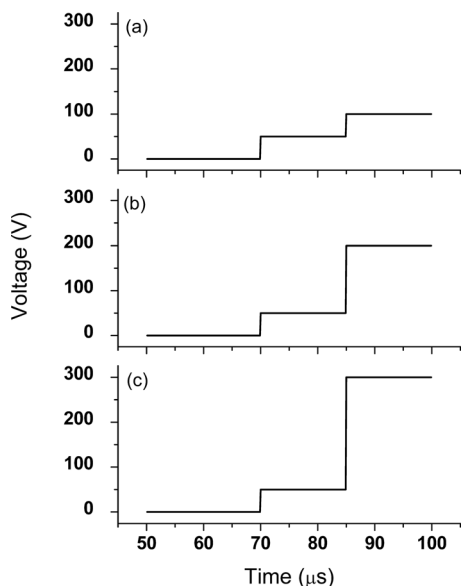

FIG. 7. Staircase DC voltage applied in the afterglow. Time $t = 50$ μs refers to the start of the afterglow (Plasma OFF). A 50 V DC step was applied starting 20 μs into the afterglow (at $t = 70$ μs), followed by the application of (a) 100 V step, (b) 200 V step, and (c) 300 V step, 15 μs later, until the end of the afterglow ($t = 100$ μs). The pressure was 10 mTorr and the gas temperature was 500 K.
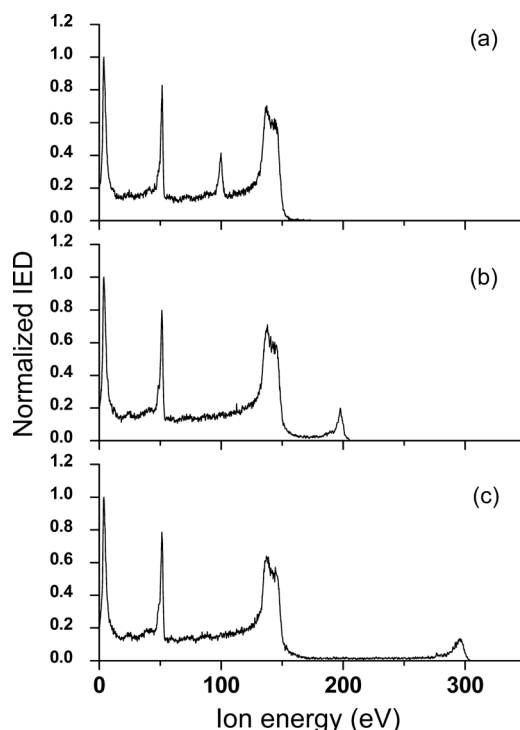

FIG. 8. Normalized ion energy distributions corresponding to the voltages of Fig. 7.

the afterglow. The IEDs corresponding to pressure of 10, 20, and 40 mTorr are shown in Figs. 9 and 10, and 11, respectively. As pressure increases, collisions become more frequent, broadening the peaks of the distribution and increasing the fraction of ions that populate the tails to the
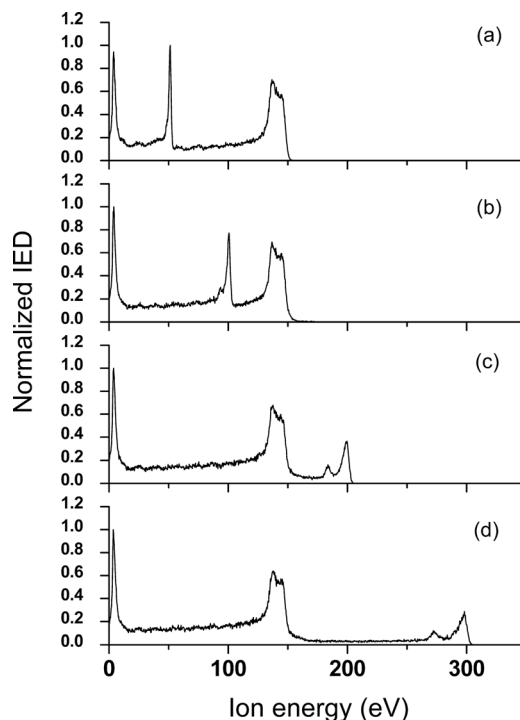

FIG. 9. Ion energy distributions for a pressure of 10 mTorr for DC bias of (a) 50V, (b) 100V, (c) 200V, and (d) 300V. The single step DC bias was applied starting at 20 μs into the afterglow ($t = 70$ μs) until the end of the afterglow. The gas temperature was 500 K.
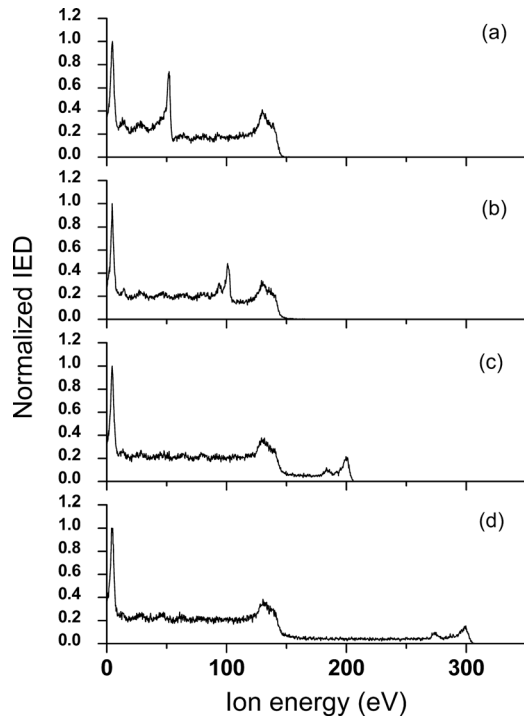
FIG. 10. Ion energy distributions for a pressure of 20 mTorr for DC bias of (a) 50 V, (b) 100 V, (c) 200 V, and (d) 300 V. The single step DC bias was applied starting at 20 μs in the afterglow ($t = 70$ μs) until the end of the afterglow. The gas temperature was 500 K.

left of the peaks. For given pressure, as voltage increases the sheath becomes thicker, making collisions more likely. At a pressure of 40 mTorr the IED has no distinct peaks except for the very low energy peak, corresponding to ions bom-
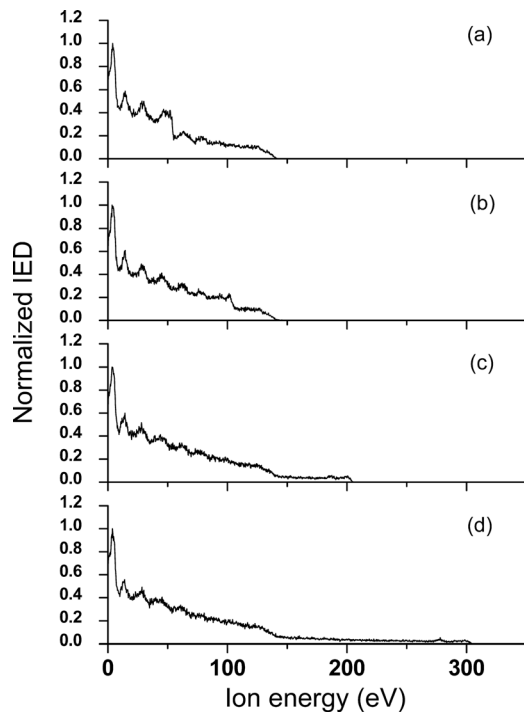

FIG. 11. Ion energy distributions for a pressure of 40 mTorr for DC bias of (a) 50 V, (b) 100 V, (c) 200 V, and (d) 300 V. The single step DC bias was applied starting at 20 μs in the afterglow ($t = 70$ μs) until the end of the afterglow. The gas temperature was 500 K.

barding the substrate during the part of the afterglow without DC bias.

In Figs. 9(c) and 9(d) and 10(c) and 10(d) two secondary peaks with energy slightly lower than 200 eV and 300 eV, can be observed. These are due to ions collected at the beginning of the application of the respective DC bias (at $t = 70$ μs and 85 μs) and correspond to the transient sheath expansion (see also Fig. 16 later) and the rise of the plasma potential. Ions striking the electrode during this transient do not manage to reach the energy of the full DC bias. These secondary peaks were present every time at the start of the application of a DC voltage, even though there were not always discernible due to overlap with the corresponding principal peak. They were clearly seen when ion-neutral collisions were intentionally turned off.

3. Effect of DC bias on plasma dynamics

The effect of applying a DC bias on the plasma dynamics is now examined. Figure 12 shows the electron density, at the discharge center, as a function of time during a power pulse. The applied bias corresponds to Fig. 7(c). During the active glow (0–50 μs), the electron density increases. As soon as the plasma power is turned OFF at $t = 50$ μs (start of afterglow), the electron density decays rather slowly (time constant of ~30 μs). Application of a 50 V bias 20 μs into the afterglow (at $t = 70$ μs), followed by a 300 V DC bias applied 35 μs into the afterglow (at $t = 85$ μs) have no perceptible effect in the density decay curve. The corresponding electron energy probability functions (EEPFs) are shown in Fig. 13. The application of 300 V DC modifies the EEPF from a bi-Maxwellian with a cold tail to a bi-Maxwellian with a hot tail. The EEPF is heated during the ramp up of the DC bias by the expanding sheath (see below). Electron heating in the tail of the EEPF over this short transient, however, hardly affects the peak electron density. There was a perceptible but not as significant change in the EEPF immediately following the application of 50 V DC as well (not shown).
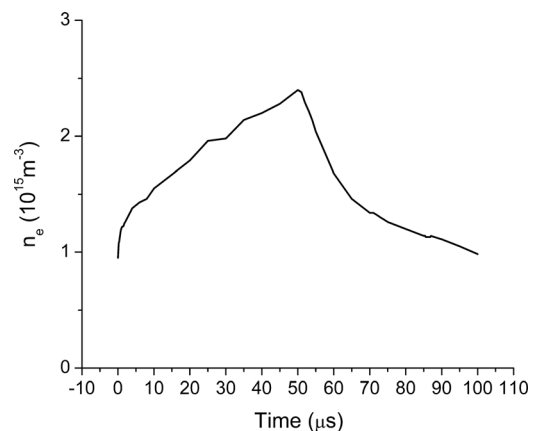

FIG. 12. Electron number density at the discharge center as a function of time for a 50 V DC bias applied at $t = 70$ μs, followed by a 300 V DC applied at $t = 85$ μs until the end of the afterglow. Time $t = 0$ refers to the start of the active glow (plasma ON). The pressure was 10 mTorr and the gas temperature was 500 K.
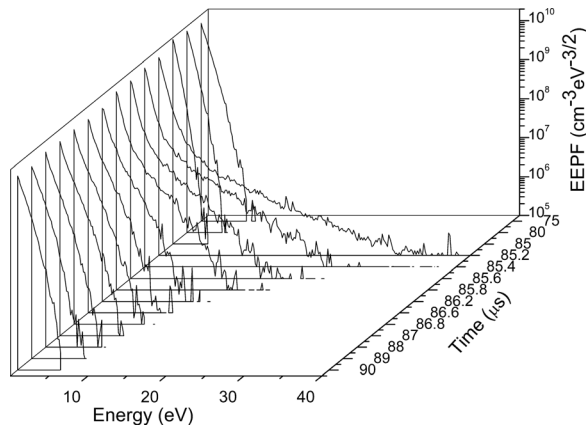
FIG. 13. Electron energy probability function at the discharge center for different times around the switch ON of the 300 V DC bias of Fig. 7(c).

FIG. 15. Electron density profiles between the parallel plates as a function of time in the afterglow. Plasma power was turned OFF at $t = 50$ μs. At $t = 70$ μs a 50 V DC bias was applied until $t = 85$ μs, when the DC bias voltage was raised to 300 V, for the rest of the afterglow (until $t = 100$ μs). The pressure was 10 mTorr and the gas temperature was 500 K. The grounded electrode is at $x = 0.06$ m.

Figure 14 shows the potential at the discharge center during a cycle of the pulsed plasma. 13.56 MHz power is turned ON at $t = 0$, and OFF at $t = 50$ μs. At $t = 70$ μs a 50 V DC bias is applied until $t = 85$ μs, when the DC bias voltage is raised to 300 V, for the rest of the afterglow (until $t = 100$ μs). During plasma power ON (0–50 μs), the bulk plasma potential is about one-half of the applied peak voltage. After power OFF, the potential collapses within microseconds to a very low value above ground. After the application of the DC boundary voltage, the potential is rapidly raised to slightly above the applied DC. It is the space potential next to the grounded substrate electrode that determines the sheath voltage over that electrode. Because of the small potential drop in the bulk plasma ($\sim$ few T_e), the sheath voltage over the substrate electrode is approximately equal to the potential shown in Fig. 14. The potential temporarily overshoots the applied DC but ions are too massive to respond to such a rapid change.

Figure 15 shows the spatial distribution of the electron density in the afterglow. Time $t = 50$ μs corresponds to power turn OFF (beginning of the afterglow). The electron density distribution assumes a diffusionlike profile within
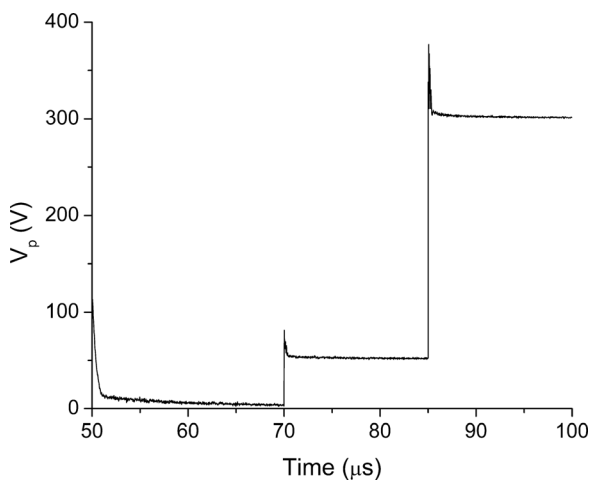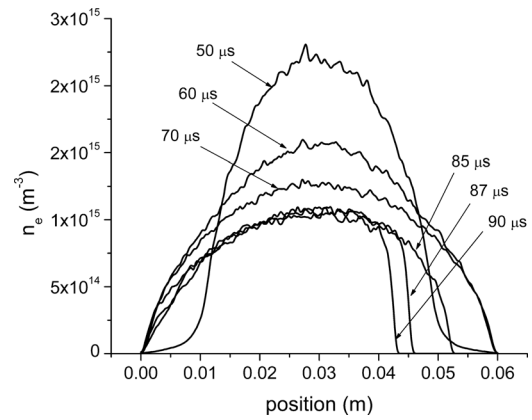
several μs into the afterglow. A 50 V DC bias is applied at 70 μs until 85 μs, when it is increased to 300 V DC until the end of the afterglow. The rise in the plasma potential V_p to slightly above 300 V generates a sheath voltage of the same magnitude over the substrate (grounded) electrode (Fig. 14).
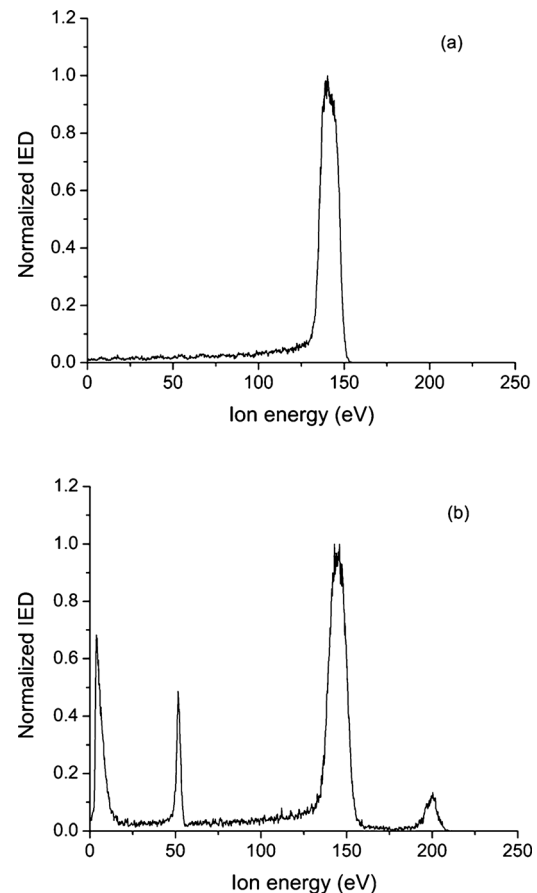

FIG 16. The case of plasma powered at 60 MHz with 300 V RF peak voltage. (a) Ion energy distribution (IED) in a continuous wave (cw) plasma. (b) IED in a pulsed plasma (50 μs power ON, 50 μs power OFF). At $t = 70$ μs a 50 V DC bias was applied until $t = 85$ μs, when the DC bias voltage was raised to 200 V, for the rest of the afterglow (until $t = 100$ μs). For both (a) and (b) the pressure was 10 mTorr and the gas temperature was 500 K.

FIG. 14. Potential at the discharge center during the afterglow. 13.56 MHz power was turned ON at $t = 0$ and OFF at $t = 50$ μs. At $t = 70$ μs a 50 V DC bias was applied until $t = 85$ μs, when the DC bias voltage was raised to 300 V, for the rest of the afterglow (until $t = 100$ μs).

This causes the sheath over the substrate to widen considerably. The sheath expansion right after the application of the DC bias, especially at 300 V, causes temporary heating of the EEPF as discussed above.

C. Plasma power at 60 MHz

The peak of the IED due to the plasma ON phase of the cycle can be made shaper by increasing the frequency of the plasma power source. This is shown in Fig. 16 where 60 MHz power was used instead of 13.56 MHz. For the same pressure and applied peak voltage, the plasma density scales with the square of the applied frequency [p. 410 of Ref. 1]. The estimated peak density is $(2.5 \times 10^9) \times (60/13.56)^2 = 5 \times 10^{10}$ cm^{-3}, the same as predicted by the PIC-MCC simulation. The higher plasma density results in thinner sheath, yet τ_i/τ_{rf} increases to ~33, resulting in narrower IED. Due to the thinner sheath, the ion collision probability is reduced, making the tail of the IED to the left of the peak less pronounced. Application of a two-level DC bias voltage in the afterglow of a pulsed discharge yields two new well-defined peaks superimposed on the peaks of the pulsed discharge without DC bias, similar to the 13.56 MHz case. The important fact is that, in both cases, the peak location and magnitude can be selected *a priori*.

IV. CONCLUSIONS

A Particle-In-Cell simulation, including Monte Carlo Collisions (PIC-MCC), was conducted of the application of tailored DC voltage steps, in the afterglow of a capacitively-coupled argon plasma, to control the ion energy distribution (IED) on the substrate electrode. IEDs with distinct energy peaks at controlled location, spacing, and fraction of ions under each peak, were obtained by judicious selection of the voltage levels and duration of a staircase DC voltage. The IED peaks displayed a tail toward lower energies due to ion-neutral collisions in the sheath. Smearing of the peaks was very pronounced at higher pressures over the range of 10–40 mTorr studied. Application of a DC voltage step resulted in temporary heating of electrons as the sheath expanded into the plasma. Under these conditions, the electron energy probability function turned temporarily from almost Maxwellian to bi-Maxwellian, with an extended energy tail. However, such electron heating, over a short transient, had no appreciable effect on the electron density decay with time in the afterglow.

[1]M. A. Lieberman and A. J. Lichtenberg, *Principles of Plasma Discharges and Materials Processing*, 2nd ed. (Wiley, Hoboken, NJ, 2005).
[2]E. Kawamura, V. Vahedi, M. A. Lieberman, and C. K. Birdsall, Plasma Sources Sci. Technol. **8**, R45 (1999).
[3]T. Panagopoulos and D. J. Economou, J. Appl. Phys. **85**, 3435 (1999).
[4]E. A. Edelberg and E. S. Aydil, J. Appl. Phys. **86**, 4799 (1999).
[5]C. Wild and P. Koidl, Appl. Phys. Lett. **54**, 505 (1989).
[6]M. M. Paterson, H.-Y. Chen, and A. E. Wendt, Plasma Sources Sci. Technol. **16**, 257 (2007).
[7]F. L. Buzzi, Y.-H. Ting, and A. E. Wendt, Plasma Sources Sci. Technol. **18**, 025009 (2009); X. V. Qin, Y.-H. Ting and A. E. Wendt, *ibid*. **19**, 065014 (2010).
[8]P. Kudlacek, R. F. Rumphorst, and M. C. M. van de Sanden, J. Appl. Phys. **106**, 073303 (2009).
[9]A. Agarwal and M. J. Kushner, J. Vac. Sci. Technol. A **23**, 1440 (2005).
[10]S. Rauf, J. Appl. Phys. **92**, 2984 (2002).
[11]V. Vahedi, G. DiPeso, C. K. Birdsall, M. A. Lieberman, and T. D. Rognlien, Plasma Sources Sci. Technol. **2**, 261 (1993); J. P. Verboncoeur, M. V. Alves, V. Vahedi and C. K. Birdsall, J. Comp. Phys. **104**, 32 (1993).
[12]V. Vahedi and M. Surendra, Comput. Phys. Commun. **87**, 179 (1995).
[13]C. K. Birdsall and A. B. Langdon, *Plasma Physics via Computer Simulation* (McGraw-Hill, New York, 1985).
[14]S. K. Nam, D. J. Economou, and V. M. Donnelly, Plasma Sources Sci. Technol. **16**, 90 (2007).
[15]L. Xu, D. J. Economou, V. M. Donnelly and P. Ruchhoeft, Appl. Phys. Lett. **87**, 041502 (2005).